UNIVERSITY OF BRISTOL

University of Bristol - Explore Bristol Research
General rights

Supplementary Information for:

Stabilisation of Water-in-Water Emulsions by Montmorillonite Platelets

William J. Ganley, Paul T. Ryan and Jeroen S. van Duijneveldt

21st April 2017

1 Interfacial Tension of the Water/Water Interface

The interfacial tension along the tie-line was measured using the droplet shape relaxation method [1, 2] where a Pu/PEO solution is allowed to equilibrate for 24 hours and then hand shaken to form Pu droplets inside a PEO continuous phase. The Pu/PEO composition tested was 6/7.6% wt. which separated into a 20% wt. Pu-rich phase and an 11% wt. PEO-rich phase (see figure 2 in the main text). A small volume of this emulsion was then placed between a microscope slide and cover slip and the slip gently pushed to shear the sample momentarily. The shape of the deformed droplet was then recorded using a microscope and camera and the relaxation of the droplet long axis L relative the spherical diameter after the droplet is fully relaxed L_0 was plotted (see figure S1).

The relaxation process is expected to follow the relationship [1, 2]:

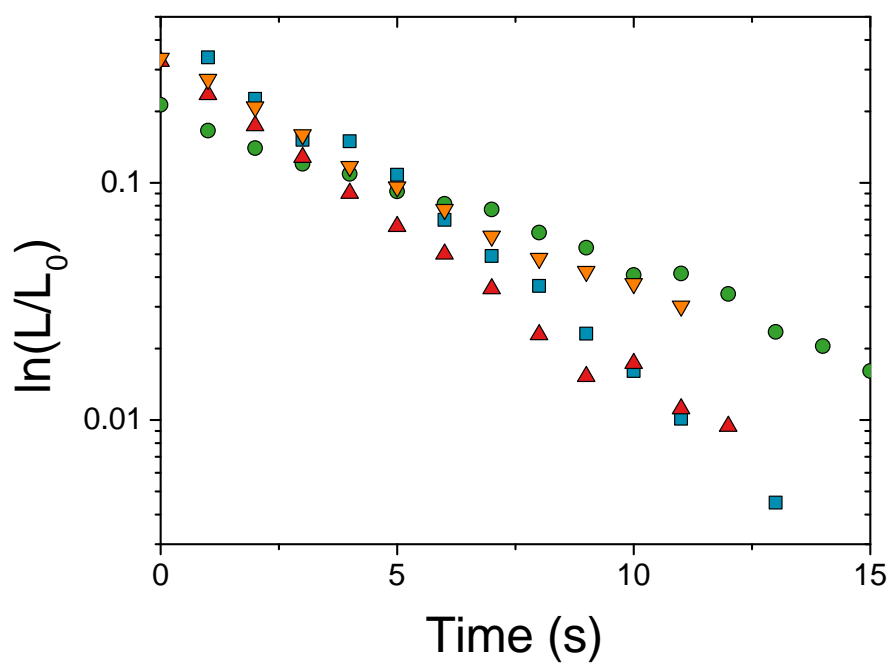$$\ln \frac{L}{L_0} \propto e^{\frac{-t}{\tau}} \tag{S1}$$

Figure S1: Relative change in largest length scale of four deformed droplets over time. Used to measure capillary time of Pu/PEO interface. Pu and PEO concentrations were 6 and 7.6% wt. respectively.

where t is the time and τ is a characteristic relaxation time which is related to the droplet capillary time (τ_{Ca}) as follows:

$$\tau = \tau_{Ca}\frac{(19K+16)(2K+3)}{40(K+1)} \tag{S2}$$

where $K = \eta_d/\eta_m$ is the viscosity ratio between the droplet and continuous phases which were taken as the ratio of low shear viscosities measured by steady state viscometry shown in figure S2. Note that the concentrations tested correspond to the equilibrium compositions of the separated phases along the tie-line (see figure 2 in the main text).
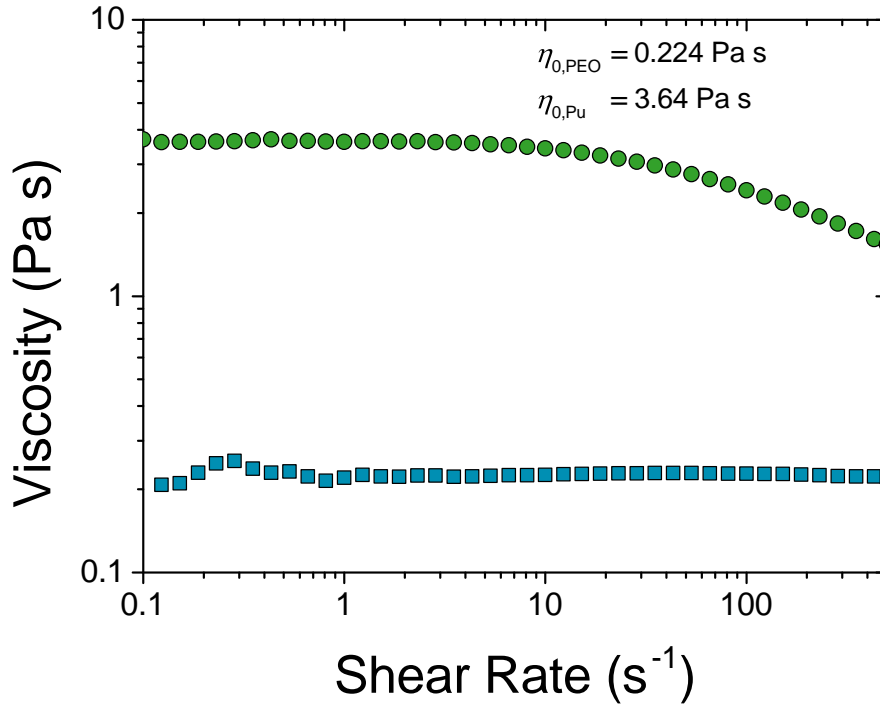

Figure S2: Equilibrium flow curves of Pu (20% wt.) and PEO solutions (11% wt.).

The capillary time measured in this way is related to the interfacial tension Γ_{AB} by

$$\tau_{Ca} = \frac{\eta_m r_0}{\Gamma_{AB}} \tag{S3}$$

where r_0 is the spherical droplet radius.

Equations S1 to S3 were used to calculate the interfacial tension of four droplets from the same phase separated mixture and these values are shown in table S1. The average interfacial tension along the tie line of figure 2 in the main text is $98\pm13\,\mu\mathrm{Nm}^{-1}$ where the uncertainty is the standard error of the mean.

τ (s)	r_0 (μm)	τ_{Ca} (s)	γ ($\mu\mathrm{Nm}^{-1}$)
2.78	76.1	0.167	102
6.44	110	0.386	63.6
3.16	105	0.189	124
4.10	110	0.245	100

Table S1: Parameters calculated from fitting equation S1 to data in figure S1 and applying equations S2 and S3.

2 Microscopy of Emulsions over Time

Figures S3 and S4 show micrographs of the emulsions sealed between a microscope slide and cover slip. These were used to measure droplet sizes shown in the histograms in figures S5 and S6 below and figure 7 in the main text.
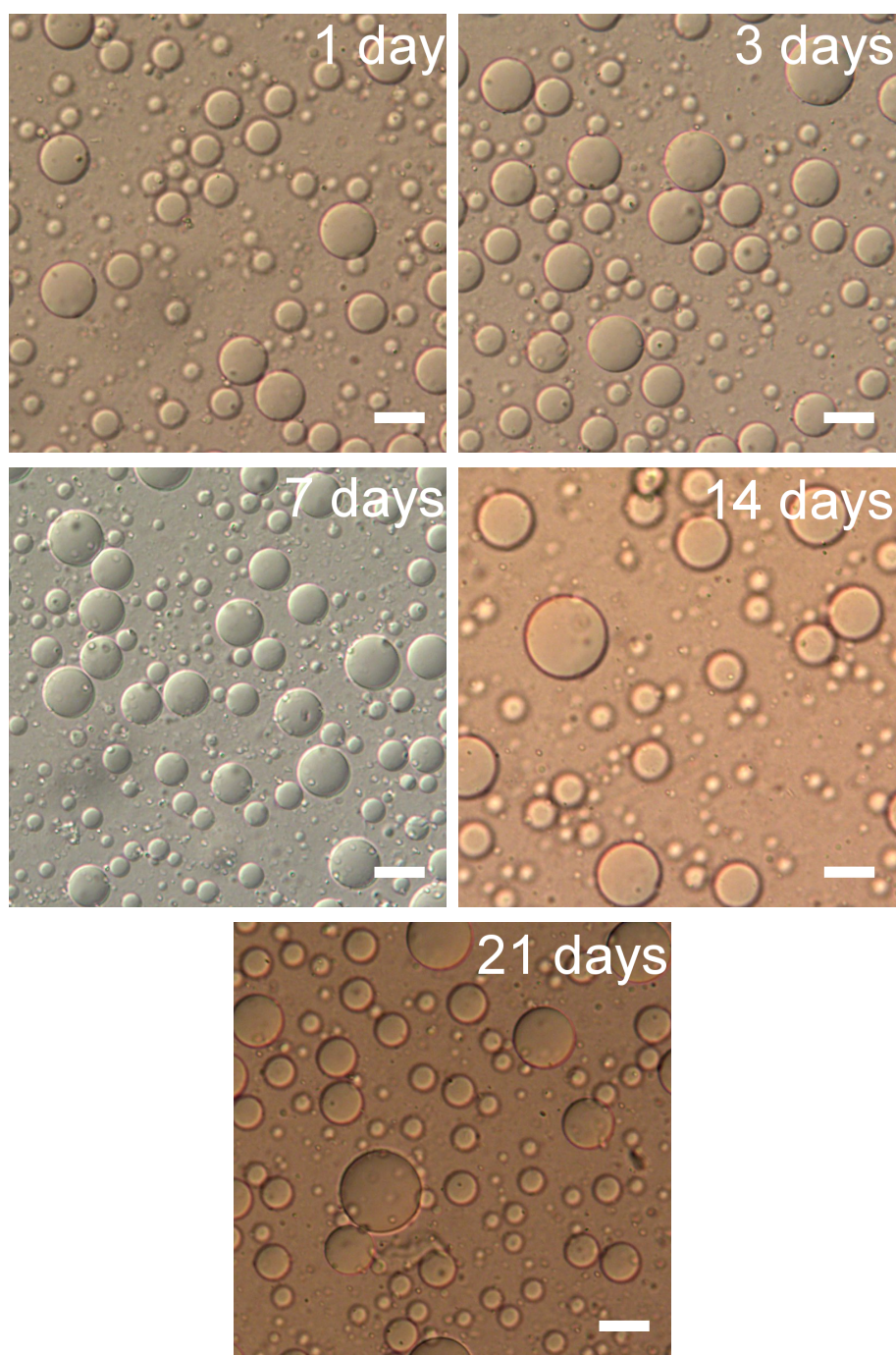
Figure S3: Differential interference contrast microscopy of 10/90 pullulan-in-polyethlene oxide emulsions over course of stability experiment. Scale bars represent 20 μm.
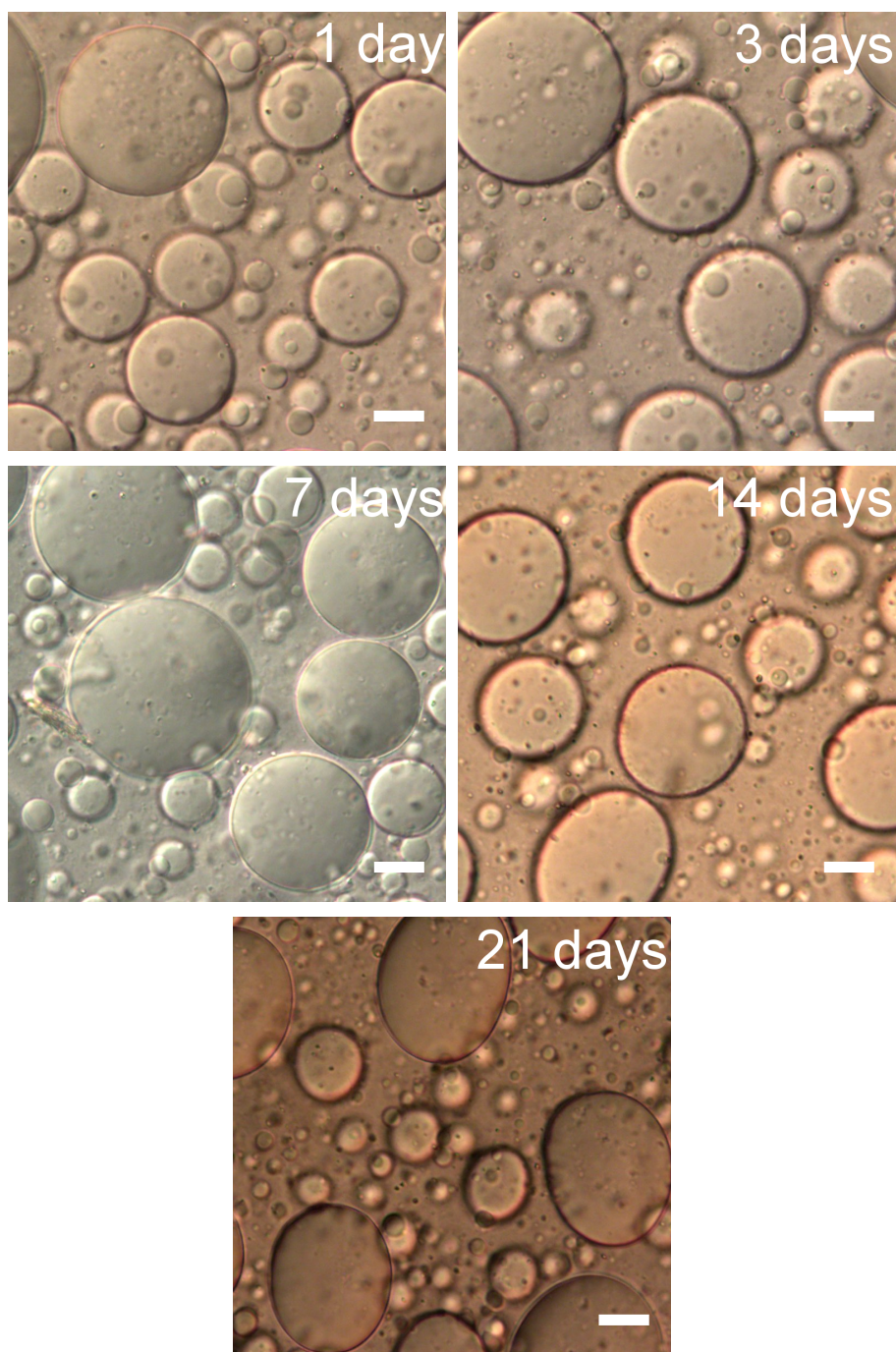
Figure S4: Differential interference contrast microscopy of 30/70 pullulan-in-polyethlene oxide emulsions over course of stability experiment. Scale bars represent 20 μm.

3 Droplet Size Histograms

Figures S5 and S6 show droplet size histograms corresponding to data points in figure 7 in the main text. At least 100 droplets were measured for each with the help of the Linear Intercept software package (TU Darmstadt).
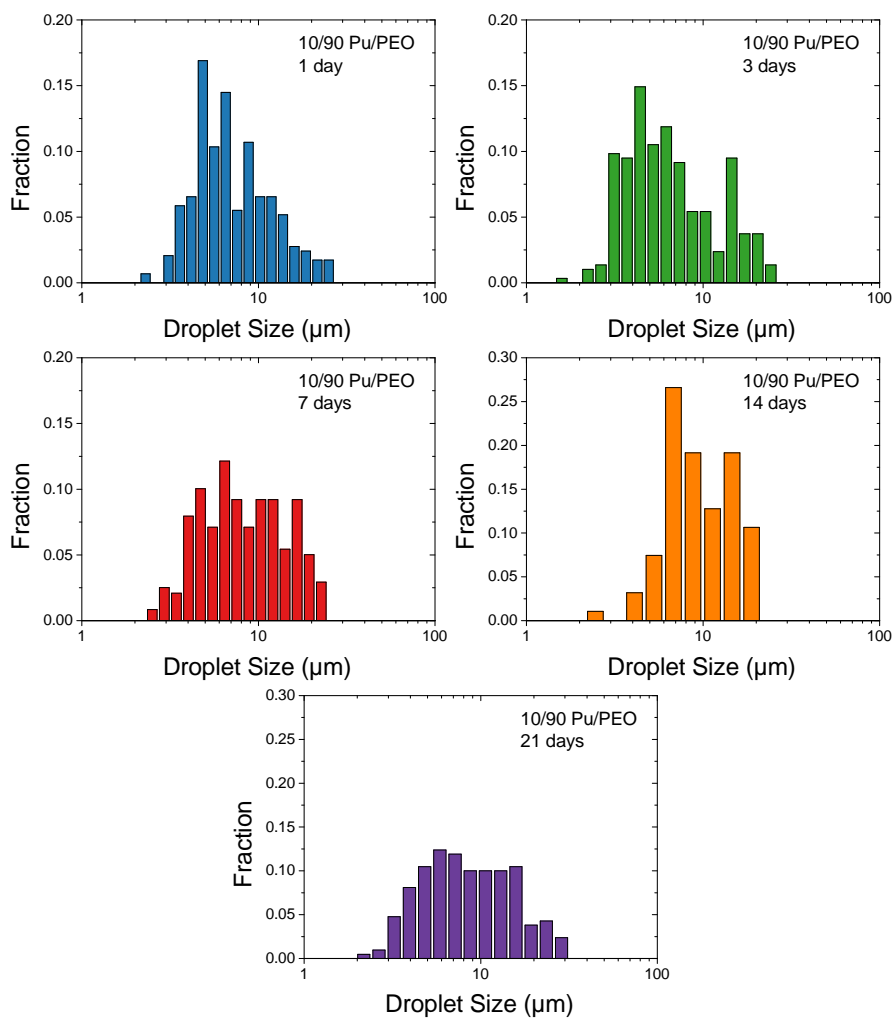
Figure S5: Droplet size histograms for 10/90 pullulan-in-polyethylene oxide emulsions.
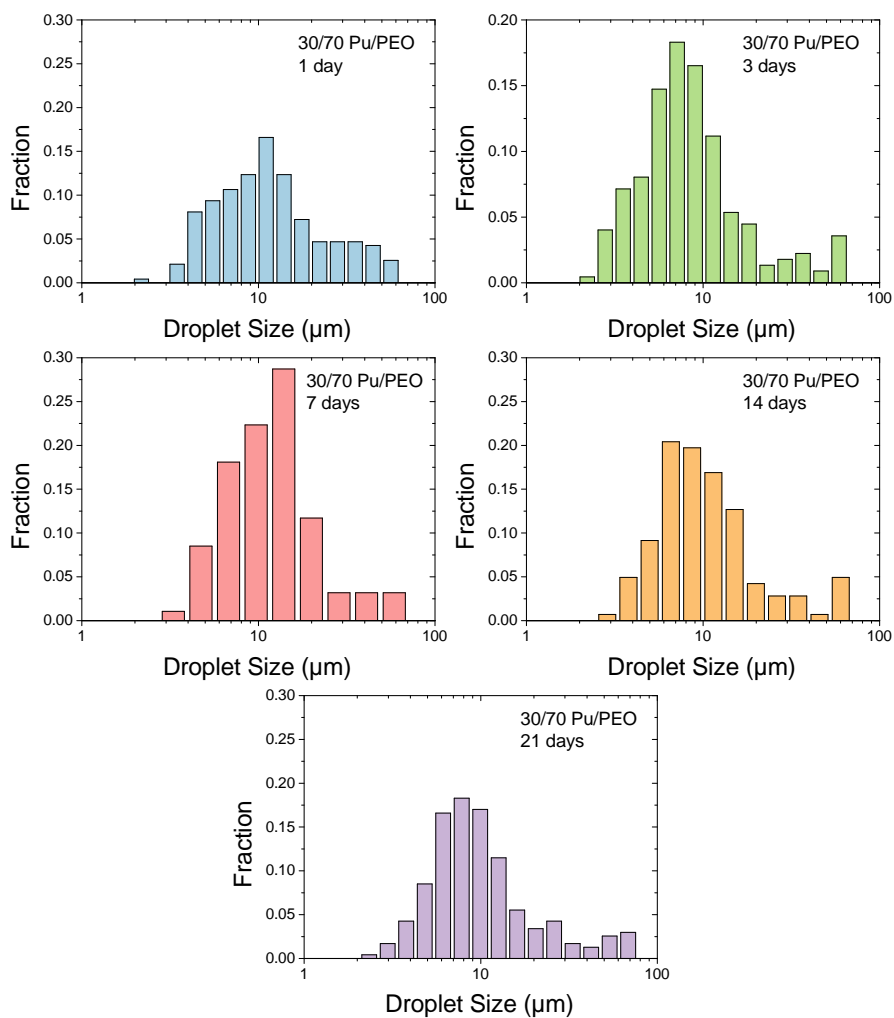
Figure S6: Droplet size histograms for 30/70 pullulan-in-polyethylene oxide emulsions.

4   Polarising Optical Microscopy Comparison of Pu-in-PEO Emulsion and Montmorillonite Suspension

Figure S7 shows polarising optical microscopy images of a 1.4% wt. montmorillonite suspension in 0.01 M NaCl and the 30/70 Pu-in-PEO emulsions shown in figure 6 of the main text. The montmorillonite suspension has the same clay concentration as the continuous phase of the emulsion. The contrast of both images have been enhanced to the same degree. There is some birefringent material in the clay suspension which could be aggregates or some small mineral impurities. In the emulsion there is much more birefringent material suggesting that the presence of the polymers results in the extensive formation of aggregate structures that have some local ordering as discussed in the main text and that this is significantly different to what is observed in absence of the polymers.
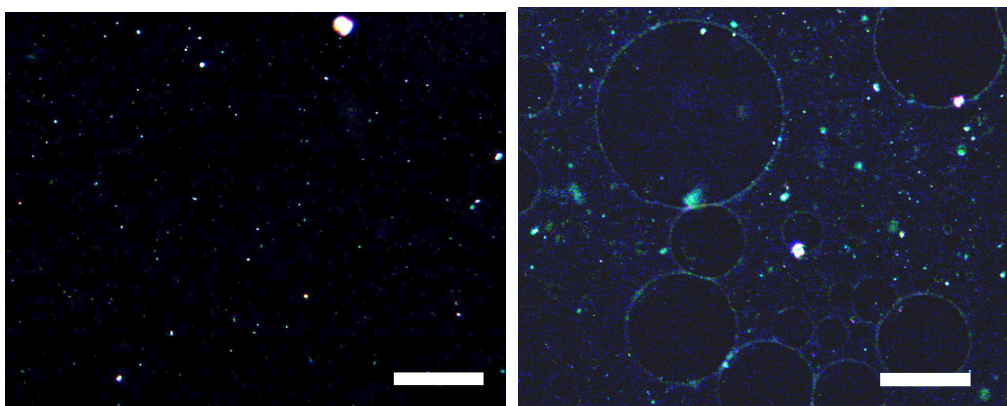

Figure S7: Polarising optical microscopy of 1.4% wt. montmorillonite suspension in 0.01 M Nacl (left) and 30/70 Pu-in-PEO emulsion. The clay concentration in the suspension is the same as in the continuous phase of the emulsion. Contrast has been enhanced in both images to the same degree. Scale bars represent 40 μm.

10

5   Photographs of the 70/30 emulsion

Figure S8 shows photographs of the 70/30 Pu/PEO emulsion discussed in section 3.3 in the main text. The upper PEO-rich phase begins to separate within the first 10 minutes however it is unclear whether this is due to droplet coalescence or the unsuccessful emulsification. In contrast to the 10/90, 30/70 and 50/50 Pu/PEO emulsions shown in figure 5 of the main text the particles here are in the lower phase. This may indicate that the PEO-rich droplets could not be broken up due to the high viscosity of the Pu-rich phase. The resulting low interfacial area combined with the high viscosity of the Pu-rich phase may have prevented the particles from migrating into the PEO-rich phase as they did in the lower Pu concentration emulsions. These combined factors are likely the reason that PEO-in-Pu emulsions could not be prepared by this method.
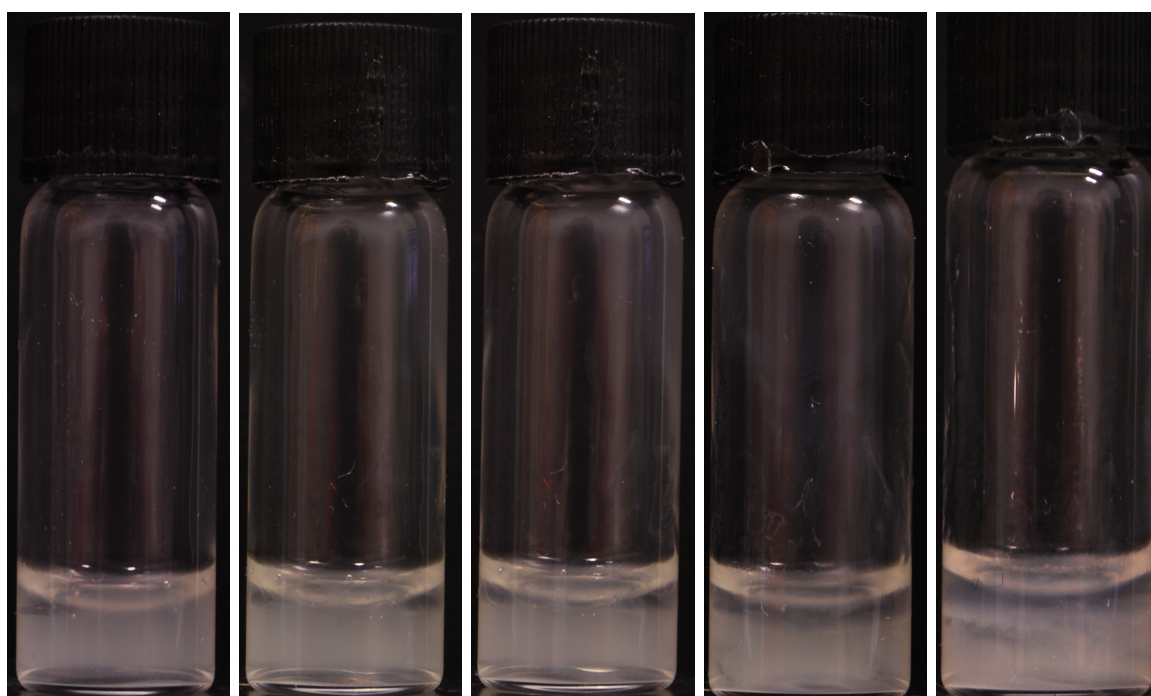
Figure S8: Photogtaphs of 70/30 Pu/PEO emulsion from left to right: immediately after preparation, after 10 minutes, 30 minutes, 2 hours and 48 hours.

References

[1] W. J. Frith, *Adv. Colloid Interface Sci.* **161**, 48 (2010).

[2] G. Balakrishnan, T. Nicolai, L. Benyahia, D. Durand, *Langmuir* **28**, 5921 (2012).